Measurement of the Λ_c^+ Lifetime

F. Abudinén, L. Aggarwal, H. Ahmed, J. K. Ahn, H. Aihara, N. Akopov, A. Aloisio, N. Anh Ky, D. M. Asner, H. Atmacan, T. Aushev, V. Aushev, V. Babu, H. Bae, P. Bambade, Sw. Banerjee, S. Bansal, J. Baudot, M. Bauer, A. Baur, A. Beaubien, J. Becker, J. V. Bennett, E. Bernieri, F. U. Bernlochner, V. Bertacchi, M. Bertemes, E. Bertholet, M. Bessner, S. Bettarini, V. Bhardwaj, F. Bianchi, T. Bilka, D. Biswas, D. Bodrov, A. Bolz, G. Bonvicini, A. Bozek, M. Bračko, P. Branchini, R. A. Briere, T. E. Browder, A. Budano, S. Bussino, M. Campajola, L. Cao, G. Casarosa, C. Cecchi, M.-C. Chang, P. Chang, R. Cheaib, P. Cheema, C. Chen, Y. Q. Chen, Y.-T. Chen, B. G. Cheon, K. Chilikin, K. Chirapatpimol, H.-E. Cho, K. Cho, S.-J. Cho, S.-K. Choi, S. Choudhury, D. Cinabro, L. Corona, L. M. Cremaldi, S. Cunliffe, F. Dattola, E. De La Cruz-Burelo, S. A. De La Motte, G. De Nardo, M. De Nuccio, G. De Pietro, R. de Sangro, M. Destefanis, A. De Yta-Hernandez, R. Dhamija, A. Di Canto, F. Di Capua, J. Dingfelder, Z. Doležal, I. Domínguez Jiménez, T. V. Dong, M. Dorigo, K. Dort, D. Dossett, S. Dreyer, G. Dujany, M. Eliachevitch, D. Epifanov, P. Feichtinger, T. Ferber, D. Ferlewicz, T. Fillinger, G. Finocchiaro, K. Flood, A. Fodor, F. Forti, A. Frey, B. G. Fulsom, A. Gabrielli, E. Ganiev, M. Garcia-Hernandez, A. Gaz, A. Gellrich, G. Ghevondyan, R. Giordano, A. Giri, A. Glazov, B. Gobbo, R. Godang, P. Goldenzweig, W. Gradl, S. Granderath, D. Greenwald, T. Gu, Y. Guan, K. Gudkova, J. Guilliams, S. Halder, K. Hara, O. Hartbrich, K. Hayasaka, H. Hayashii, S. Hazra, C. Hearty, I. Heredia de la Cruz, M. Hernández Villanueva, A. Hershenhorn, T. Higuchi, M. Hohmann, T. Humair, T. Iijima, K. Inami, G. Inguglia, N. Ipsita, A. Ishikawa, S. Ito, R. Itoh, M. Iwasaki, Y. Iwasaki, P. Jackson, W. W. Jacobs, D. E. Jaffe, Q. P. Ji, Y. Jin, H. Junkerkalefeld, M. Kaleta, J. Kandra, K. H. Kang, R. Karl, G. Karyan, C. Kiesling, C.-H. Kim, D. Y. Kim, K.-H. Kim, Y.-K. Kim, H. Kindo, K. Kinoshita, P. Kodyš, T. Koga, S. Kohani, K. Kojima, A. Korobov, S. Korpar, E. Kovalenko, R. Kowalewski, T. M. G. Kraetzschmar, P. Križan, P. Krokovny, T. Kuhr, J. Kumar, R. Kumar, K. Kumara, T. Kunigo, Y.-J. Kwon, S. Lacaprara, T. Lam, L. Lanceri, J. S. Lange, M. Laurenza, R. Leboucher, S. C. Lee, P. Leitl, D. Levit, L. K. Li, S. X. Li, Y. B. Li, J. Libby, Z. Liptak, Q. Y. Liu, D. Liventsev, S. Longo, T. Lueck, C. Lyu, M. Maggiora, R. Maiti, S. Maity, R. Manfredi, E. Manoni, S. Marcello, C. Marinas, L. Martel, A. Martini, L. Massaccesi, M. Masuda, K. Matsuoka, D. Matvienko, J. A. McKenna, F. Meier, M. Merola, M. Milesi, C. Miller, K. Miyabayashi, G. B. Mohanty, N. Molina-Gonzalez, S. Moneta, H. Moon, H.-G. Moser, M. Mrvar, R. Mussa, I. Nakamura, M. Nakao, H. Nakayama, A. Narimani Charan, M. Naruki, Z. Natkaniec, A. Natochii, L. Nayak, M. Nayak, G. Nazaryan, C. Niebuhr, N. K. Nisar, S. Nishida, K. Nishimura, H. Ono, P. Oskin, E. R. Oxford, G. Pakhlova, A. Paladino, A. Panta, E. Paoloni, S. Pardi, K. Parham, H. Park, S.-H. Park, A. Passeri, T. K. Pedlar, I. Peruzzi, R. Peschke, R. Pestotnik, F. Pham, L. E. Piilonen, G. Pinna Angioni, P. L. M. Podesta-Lerma, T. Podobnik, S. Pokharel, L. Polat, C. Praz, S. Prell, E. Prencipe, M. T. Prim, H. Purwar, N. Rad, P. Rados, S. Raiz, M. Reif, S. Reiter, I. Ripp-Baudot, G. Rizzo, S. H. Robertson, J. M. Roney, A. Rostomyan, N. Rout, G. Russo, D. A. Sanders, S. Sandilya, A. Sangal, L. Santelj, Y. Sato, V. Savinov, B. Scavino, C. Schwanda, A. J. Schwartz, Y. Seino, A. Selce, K. Senyo, J. Serrano, C. Sfienti, C. P. Shen, T. Shillington, J.-G. Shiu, A. Sibidanov, F. Simon, R. J. Sobie, A. Soffer, A. Sokolov, E. Solovieva, S. Spataro, B. Spruck, M. Starič, S. Stefkova, R. Stroili, J. Strube, M. Sumihama, K. Sumisawa, W. Sutcliffe, S. Y. Suzuki, H. Svidras, M. Takahashi, M. Takizawa, U. Tamponi, S. Tanaka, K. Tanida, H. Tanigawa, N. Taniguchi, F. Tenchini, R. Tiwary, D. Tonelli, E. Torassa, N. Toutounji, K. Trabelsi, M. Uchida, K. Unger, Y. Unno, K. Uno, S. Uno, P. Urquijo, Y. Ushiroda, S. E. Vahsen, R. van Tonder, G. S. Varner, K. E. Varvell, A. Vinokurova, L. Vitale, V. Vobbilisetti, E. Waheed, H. M. Wakeling, E. Wang, M.-Z. Wang, X. L. Wang, A. Warburton, S. Watanuki, M. Welsch, C. Wessel, J. Wiechczynski, H. Windel, E. Won, X. P. Xu, B. D. Yabsley, S. Yamada, S. B. Yang, H. Ye, J. Yelton, J. H. Yin, K. Yoshihara, Y. Yusa, Y. Zhang, V. Zhilich, Q. D. Zhou, V. I. Zhukova, and R. Žlebčík

(The Belle II Collaboration)

(Received 29 June 2022; accepted 25 July 2022; published 16 February 2023)

An absolute measurement of the Λ_c^+ lifetime is reported using $\Lambda_c^+ \to pK^-\pi^+$ decays in events reconstructed from data collected by the Belle II experiment at the SuperKEKB asymmetric-energy electron-positron collider. The total integrated luminosity of the data sample, which was collected at center-of-mass energies at or near the $\Upsilon(4S)$ resonance, is 207.2 fb^{-1}. The result, $\tau(\Lambda_c^+) = 203.20 \pm 0.89 \pm 0.77$ fs, where the first uncertainty is statistical and the second systematic, is the most precise measurement to date and is consistent with previous determinations.

DOI: 10.1103/PhysRevLett.130.071802

Searches for physics beyond the standard model of particle physics through precise measurements of weakly decaying charm or bottom hadrons often rely on accurate theoretical descriptions of strong interactions at low energy, typically using effective models such as the heavy quark expansion (HQE) [1–7]. The HQE provides a consistent framework for computing the decay widths of heavy hadrons in terms of inverse powers of the heavy quark mass. For bottom hadrons, nonperturbative effects are relatively small, and the HQE in $1/m_b$, where m_b is the mass of the bottom quark, works well. In contrast, higher-order corrections due to the influence of light valence (spectator) quarks are significant for charm hadron lifetimes, for which the HQE to $1/m_c^3$ does not satisfactorily describe lifetimes [7]. The lifetimes of the Ω_c^0 and Ξ_c^0 were recently measured to be much larger than the previous world average [8–10], inverting the known hierarchy of charm lifetimes. Careful consideration of model-dependent spectator effects is required for theoretical predictions of charm baryon lifetimes to agree with experimental measurements [6,7]. Improved measurements of charm baryon lifetimes therefore provide refined tests for effective models.

The world average value of the Λ_c^+ lifetime is 202.4 ± 3.1 fs [11]. Previous measurements include percent-level results from the FOCUS, SELEX, and CLEO collaborations two decades ago [12–14], as well as a more precise measurement, relative to the D^+ lifetime, from the LHCb collaboration [9]. The latter of these has a limiting systematic uncertainty associated with the D^+ lifetime. Relative measurements minimize systematic uncertainties related to event selection that may bias the decay time, particularly at hadron colliders. In contrast, the ability to reconstruct charm hadrons without biasing the decay time allows experiments at electron-positron (e^+e^-) colliders to precisely determine absolute lifetimes, as demonstrated by the recent measurement of the D^0 and D^+ lifetimes [15] from the Belle II experiment [16] at the SuperKEKB asymmetric-energy e^+e^- collider [17]. The most recent Λ_c^+ lifetime measurement at an e^+e^- collider, from the CLEO collaboration, is in mild tension with other results and increases the uncertainty of the world average [11]. A precise, absolute measurement by Belle II may help to resolve the tension between Λ_c^+ lifetime measurements at e^+e^- colliders and other experiments and will substantially improve the world average.

In this Letter, we report a precise measurement of the Λ_c^+ lifetime using $\Lambda_c^+ \to pK^-\pi^+$ decays reconstructed in data collected at or near the $\Upsilon(4S)$ resonance, corresponding to a center-of-mass energy at or near 10.58 GeV, by the Belle II experiment from 2019 to mid 2021 and corresponding to an integrated luminosity of 207.2 fb^{-1}. Unless specified otherwise, charge conjugate decays are implied throughout.

The lifetime of the Λ_c^+ is determined from a two-dimensional fit to the decay time t and its uncertainty σ_t. The decay time is calculated assuming that Λ_c^+ candidates are promptly produced from continuum $e^+e^- \to c\bar{c}$ events and is determined according to $t = m_{\Lambda_c}\vec{L}\cdot\vec{p}/|\vec{p}|^2$, where m_{Λ_c} is the world average mass of the Λ_c^+ [11], $\vec{L}$ is the displacement of the Λ_c^+ decay point from the e^+e^- interaction point (IP), and $\vec{p}$ is the momentum of the Λ_c^+ candidate. The position and size of the IP region is determined using $e^+e^- \to \mu^+\mu^-$ events. Event selection criteria and the fit strategy are optimized and validated using simulated data, but the fit to the collision data does not use any input taken from simulation.

The Belle II detector [16] includes a tracking system comprising a two-layer silicon pixel detector (PXD) surrounded by a four-layer double-sided silicon strip detector (SVD) and a 56-layer central drift chamber (CDC). The second layer of the PXD had 15% azimuthal coverage during the collection of the data used in this study. For the Λ_c^+ decays considered here, the combined PXD and SVD vertexing system provide a decay-length resolution of 40 μm, corresponding to an average decay-time resolution of 87 fs for an average decay length of 96 μm. A time-of-propagation counter in the barrel region of the detector and an aerogel ring-imaging Cherenkov counter in the endcap region provide charged-particle identification (PID) information. An electromagnetic calorimeter consisting of CsI(Tl) crystals provides energy and timing measurements for photons and electrons. A K_L^0 and muon detector is installed in the iron flux return yoke of a superconducting solenoid magnet that provides a 1.5 T magnetic field.

We generate $e^+e^- \to q\bar{q}$ events with KKMC [18] and hadronize quarks with Pythia 8 [19]. Hadron decays are emulated using EvtGen [20]. The detector response is simulated with Geant4 [21]. Reconstruction of events from simulated and collision data is performed with the Belle II analysis software framework [22]. In addition to the excellent vertexing capability, Belle II benefits from good charged-particle tracking performance [23,24].

Candidate $\Lambda_c^+ \to pK^-\pi^+$ decays are each reconstructed from one negatively and two positively charged particles, which are required to be well measured with reliable uncertainties to allow for a precise lifetime measurement. Each charged particle must be associated with one or more PXD measurements (hits) in the PXD, at least one hit in the first layer of the SVD, and at least 20 hits in the CDC. Each charged particle must have a distance of closest approach to the IP of less than 0.5 cm in the plane transverse to the beam and 2 cm in the direction parallel to it to remove charged particles not associated with the e^+e^- interaction. A fit constrains the charged particles to come from a common vertex and the Λ_c^+ candidate to come from the IP [25]. Candidates with a vertex-fit χ^2 probability less than 0.01 are rejected. Since the Λ_c^+ is assumed to originate from the IP, secondary decays in which the Λ_c^+ originates from a displaced vertex would bias the lifetime measurement. To suppress Λ_c^+ from B decays, the center-of-mass momentum of each Λ_c^+ candidate is required to be greater than 2.5 GeV/c.

Charged PID information is combined from all subdetector systems except the PXD and SVD. This PID information is used to construct likelihoods $\mathcal{L}(h)$ for a given particle hypothesis h. For each candidate, one positively charged particle is required to have $\mathcal{L}(p)/[\mathcal{L}(p)+\mathcal{L}(K)+\mathcal{L}(\pi)] > 0.9$, the negatively charged particle is required to have $\mathcal{L}(K)/[\mathcal{L}(p)+\mathcal{L}(K)+\mathcal{L}(\pi)+\mathcal{L}(\mu)+\mathcal{L}(e)+\mathcal{L}(d)] > 0.6$, and the remaining positively charged particle is assumed to be a pion. Here $\mathcal{L}(d)$ is the deuteron hypothesis likelihood. The efficiency of the proton identification is found to be about 88%, with a kaon contamination of less than 2%, and the efficiency of kaon identification is 70%, with a pion contamination of 6%, from studies of $\Lambda^0 \to p\pi^-$ and D^{*+}-tagged $D^0 \to K^-\pi^+$ decays. To reduce backgrounds from misidentified charm-meson decays, we reject events with $M(\pi^+K^-\pi^+)$ in $[1.858, 1.881]$ GeV/c^2 or $[2.000, 2.020]$ GeV/c^2, with both positively charged particles assumed to be pions. These intervals correspond to three units of resolution, or standard deviations, on the reconstructed mass in both directions around the known D^+ and D^{*+} masses, respectively. Other charm-related backgrounds are suppressed by requiring that the transverse momenta of pions exceed 0.35 GeV/c and those of protons exceed 0.7 GeV/c.

Events with multiple candidates, which occur at a rate of 0.2%, are rejected. Analysis of simulated events shows that the event selection criteria do not bias the measurement of the Λ_c^+ lifetime.

Decays of $\Xi_c^0 \to \pi^-\Lambda_c^+$ and $\Xi_c^+ \to \pi^0\Lambda_c^+$ may bias the measurement of the Λ_c^+ lifetime, since the Ξ_c^0 and Ξ_c^+ have lifetimes of 153 ± 6 fs and 456 ± 5 fs [11], respectively, and may shift the production vertex of the Λ_c^+ away from the IP. The amount of Ξ_c contamination is estimated from a fit to the distribution of the Λ_c^+ vertex displacement from the IP in the plane transverse to the beam line. This distribution depends only on the resolution of the detector for Λ_c^+ candidates that are produced at the IP. Λ_c^+ candidates from Ξ_c decays have production vertices that are displaced from the IP and therefore a larger vertex displacement from the IP. The fit to the distribution of the Λ_c^+ transverse vertex displacement gives a background contamination of 374 ± 88 events, corresponding to 0.003% of Λ_c^+ candidates. As this includes both combinatoric backgrounds and Ξ_c decays, the central value is taken as an estimate of the maximum number of Ξ_c decays. This value is consistent with predictions based on the expected production cross-sections for Ξ_c^0 and Ξ_c^+ [26], the measured branching fraction for $\Xi_c^0 \to \pi^-\Lambda_c^+$ [27], and theoretical predictions for $\Xi_c^+ \to \pi^0\Lambda_c^+$ [28]. Backgrounds from Ξ_c decays are reduced by restricting the invariant mass of the Ξ_c candidate formed by combining the Λ_c^+ candidate with a π^- or π^0 from the unassigned particle candidates of the event. This restriction is optimized using simulations, and the optimal precision on the lifetime measurement is achieved by restricting the mass difference between the Ξ_c and Λ_c^+ candidates to two units of the mass resolution, removing events with $M(pK^-\pi^+\pi^-) - M(pK^-\pi^+)$ in $[0.1834, 0.1864]$ GeV/c^2 or $M(pK^-\pi^+\pi^0) - M(pK^-\pi^+)$ in $[0.1753, 0.1873]$ GeV/c^2. About 61% of Ξ_c decays to Λ_c survive this veto, according to studies of simulated events. To account for the effect of the remaining background of this type, the measured Λ_c^+ lifetime is corrected by subtracting a bias of 0.34 fs, as discussed below.

After all selection criteria, the number of events in the Λ_c^+ signal range, defined as $M(pK^-\pi^+)$ in $[2.283, 2.290]$ GeV/c^2, within about 1.4 units of the mass resolution around the world average Λ_c^+ mass, is 1.16×10^5. The relative amount of signal events, determined from a binned least-squares fit to the $M(pK^-\pi^+)$ distribution (Fig. 1), is 92.5%. In the fit, the $\Lambda_c^+ \to pK^-\pi^+$ signal is modeled as the sum of Gaussian and Johnson functions [29] with a common mode. The background is modeled as a linear function. Events from the Λ_c^+ sidebands, defined as $M(pK^-\pi^+)$ in $[2.249, 2.264]$ GeV/c^2 and $[2.309, 2.324]$ GeV/c^2, are used to constrain the background in the lifetime fit.

The Λ_c^+ lifetime is measured with an unbinned maximum-likelihood fit to the (t, σ_t) distribution for events in the signal region. The signal probability density function (PDF) is the product of an exponential function in t

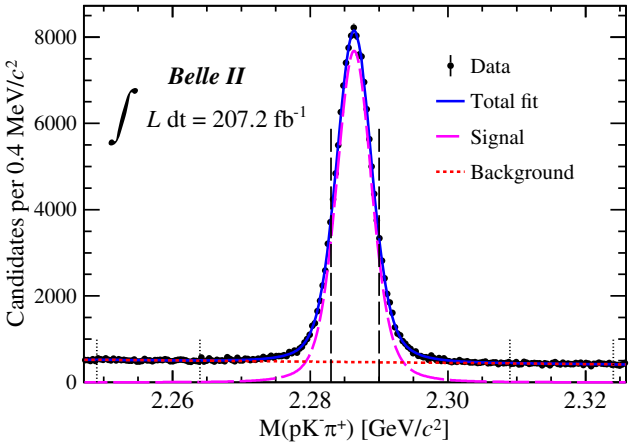

FIG. 1. Mass distribution of $\Lambda_c^+ \to pK^-\pi^+$ candidates with fit projections overlaid. The vertical dashed lines enclose the signal region, and the short, vertical dotted lines enclose the sidebands.

convolved with a Gaussian resolution function, which depends on σ_t, and a PDF for σ_t. The latter is a histogram template formed from signal candidates subtracted by the distribution of sideband candidates after scaling according to the size of the signal and background regions. To account for a possible bias in the decay-time determination, the mean of the resolution function is determined by the fit.

The background PDF, an empirical model of the sideband data, is the sum of two exponential functions convolved with Gaussian resolution functions, which account for backgrounds from long-lived particles, and a zero-lifetime component consisting only of the resolution function, which accounts for combinatorial backgrounds. To account for a possible misestimation of the decay-time uncertainty, the width of the resolution function is given by the per-candidate σ_t multiplied by a scale factor s, which is a free parameter in the lifetime fit. The mean of the resolution function is common for all terms, but a separate σ_t -scaling parameter is used for the background PDF.

To better constrain the background, a simultaneous fit to the events in the signal region and sidebands is performed, where the σ_t PDF for the sidebands is a binned template determined by sideband events. The background fraction in the lifetime fit is Gaussian constrained to $(7.50 \pm 0.02)\%$, as determined from the $M(pK^-\pi^+)$ fit.

The lifetime fit is validated both on fully simulated data equivalent to 1 ab^{-1}, about five times the integrated luminosity of the collision data, and on simulated distributions generated by randomly sampling the lifetime PDF determined from a fit to the collision data. All validation fits return unbiased results, regardless of the assumed Λ_c^+ lifetime. Studies of the decay-time distribution in simulation suggest that σ_t is underestimated by about 10%, which is in good agreement with the results from the lifetime fit to the data, for which the scale parameter is determined to be $s = 1.108 \pm 0.006$. The mean of the resolution function is determined to be 4.77 ± 0.63 fs.

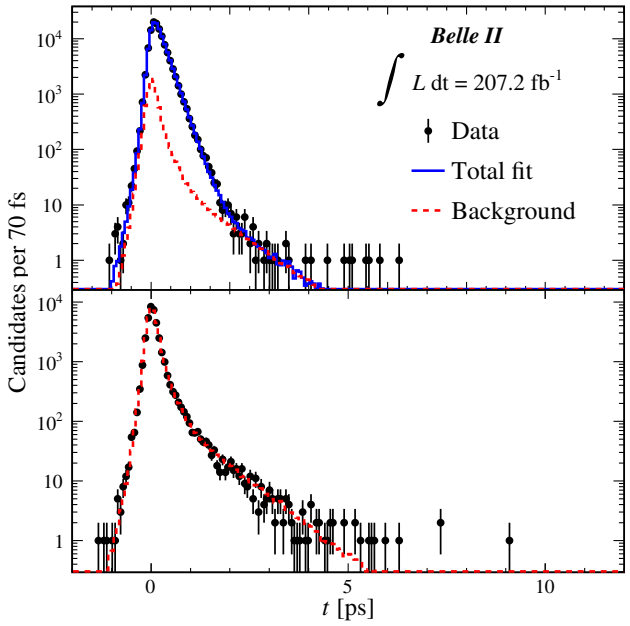

FIG. 2. Decay-time distribution of $\Lambda_c^+ \to pK^-\pi^+$ events in the signal region (top) and sidebands (bottom) with fit projections overlaid.

The Λ_c^+ lifetime is measured to be 203.20 ± 0.89 fs, where the uncertainty is statistical only. The lifetime fit projection, overlaid on the decay-time distribution in the data sample, is shown in Fig. 2. The σ_t PDF used in the lifetime fit is shown in Fig. 3. The systematic uncertainty is

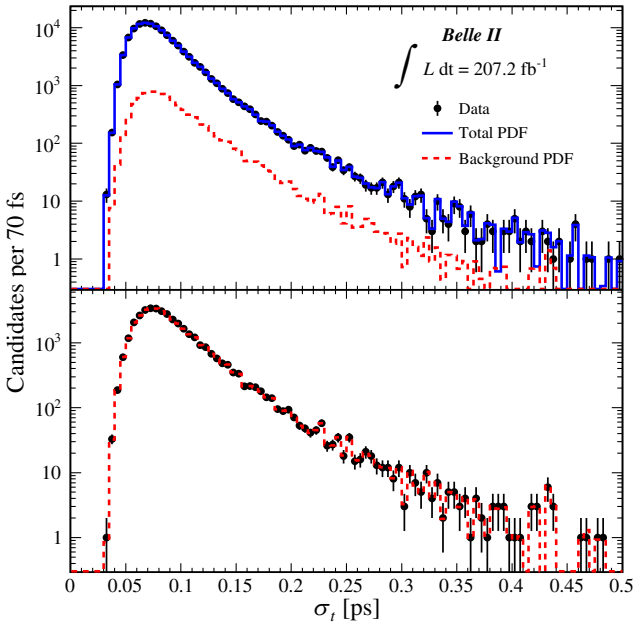

FIG. 3. Decay-time uncertainty distribution of $\Lambda_c^+ \to pK^-\pi^+$ events in the signal region (top) and sidebands (bottom). The σ_t PDF used in the fit is shown by the solid blue histogram, and the background σ_t PDF is shown by the dashed red histogram.

TABLE I. Systematic uncertainties on the Λ_c^+ lifetime.

Source	Uncertainty (fs)
Ξ_c contamination	0.34
Resolution model	0.46
Non-Ξ_c backgrounds	0.20
Detector alignment	0.46
Momentum scale	0.09
Total	0.77

calculated from the sum in quadrature of individual contributions from the sources listed in Table I and described below.

The systematic uncertainty due to backgrounds from Ξ_c decays is determined by adding simulated events of this type to the 1 ab^{-1} equivalent simulated sample according to the estimated maximum contamination determined from the fit to the distribution of the Λ_c^+ transverse vertex displacement in data and repeating the measurement. The difference between the simulated Λ_c^+ lifetime and the measured value is 0.68 fs. Since this is an estimate of the maximum effect of remaining Ξ_c backgrounds, half the difference, 0.34 fs, is taken as both a correction to the lifetime and an associated systematic uncertainty.

The resolution model for the lifetime PDF is complicated by correlations between the decay time and the decay-time uncertainty such that it cannot be described by a simple Gaussian function. We neglect these correlations in our model, which consists of a σ_t -dependent Gaussian resolution multiplied by a PDF in σ_t, and include the impact of this approximation as a systematic uncertainty. We fit our model to 1000 sets of signal-only simulated decays, each with a size equivalent to the data. The sets are produced by resampling, with repetition, simulated events in an amount corresponding to an equivalent luminosity of 1 ab^{-1}. The difference in the mean lifetime determined from these fits relative to the true value is 0.46 fs, which is taken as a systematic uncertainty due to the resolution model.

To check the resolution model, the lifetime fit is repeated with the Gaussian resolution function replaced with a sum of two Gaussian functions. The difference in the measured lifetime, 0.36 ± 0.23 fs, is covered by the corresponding systematic uncertainty. The bias of the decay-time resolution function for signal events depends on the Λ_c^+ candidate mass, but cancels if the signal range is centered on the true mass. Differences in the measured lifetime with the signal region varied are consistent with statistical fluctuations and are within the systematic uncertainty due to the resolution model.

Sideband events are included in the lifetime fit to constrain the background PDF. In simulation, sideband events describe the background distribution in the signal region accurately. To account for potential disagreements between the signal region and sidebands in the data, we produce 1000 sets of simulated data by resampling from the 1 ab^{-1}-equivalent simulated sample for events in the signal region and from the sidebands of the data sample for events in the sideband region. The mean lifetime residual is 0.20 fs, which is taken as a systematic uncertainty associated with background contamination.

To check the signal PDF for the $M(pK^-\pi^+)$ fit, we replace the sum of Gaussian and Johnson functions with a sum of two Gaussian functions. Using the resulting background contribution has a negligible effect on the measured lifetime.

Reconstruction of charged particles at Belle II relies on periodic calibrations to correct for detector misalignment and surface deformations of the internal components of the PXD and SVD, as well as for relative alignments of the tracking system [30]. Detector misalignment can bias measured particle-decay lengths and therefore their decay times. To account for imperfections in the detector alignment, sets of signal-only simulated data, each with a size comparable to the collision data, are produced with detectors randomly misaligned according to the alignment precision observed in data. The root mean square dispersion of the lifetime residuals in these misaligned simulated datasets is 0.46 fs, which is taken as a systematic uncertainty due to imperfect detector alignment.

The momenta of charged particles are scaled by a factor, 0.99971, determined by calibrating the peak positions of abundant charm, strange, and bottom hadron decays. The uncertainty on this scale factor, 0.0009, results in a systematic uncertainty on the Λ_c^+ lifetime of 0.09 fs. The uncertainty on the world average of the Λ_c^+ mass results in a negligible systematic uncertainty.

As a check of the internal consistency of the lifetime measurement, the full analysis is repeated on subsets of data chosen according to data-collection periods and Λ_c^+ momentum ranges, directions, and charge. The result for each subset is consistent with the full result. The lifetime fit is also repeated by selecting the candidate with the best vertex fit probability or randomly selecting a candidate, rather than rejecting events with multiple candidates. The difference in lifetime in each case is negligible. Finally, several events in the data have lifetimes greater than 4 ps, as shown in Fig. 2. Studies of simulated events suggest that these are from long-lived charm meson decays and show that they do not bias the lifetime result with the current dataset size.

In conclusion, we measure the Λ_c^+ lifetime to be $203.20 \pm 0.89 \pm 0.77$ fs where the first uncertainty is statistical and the second systematic, using data with an integrated luminosity of 207.2 fb^{-1} collected by the Belle II experiment at the SuperKEKB asymmetric-energy e^+e^- collider. This is consistent with the recent, relative measurement by LHCb [9] and other previous results, though the mild tension between the measurement by CLEO [14] and all other measurements remains. The absolute measurement presented here is the most precise Λ_c^+ lifetime measurement to date and may be useful to test the accuracy of HQE

models as theoretical precision improves and discrepancies between theory and experiment become more significant.

This work, based on data collected using the Belle II detector, which was built and commissioned prior to March 2019, was supported by the Science Committee of the Republic of Armenia Grant No. 20TTCG-1C010; Australian Research Council and research Grants No. DE220100462, No. DP180102629, No. DP170102389, No. DP170102204, No. DP150103061, No. FT130100303, No. FT130100018, and No. FT120100745; Austrian Federal Ministry of Education, Science and Research, Austrian Science Fund No. P 31361-N36 and No. J4625-N, and Horizon 2020 ERC Starting Grant No. 947006 "InterLeptons"; Natural Sciences and Engineering Research Council of Canada, Compute Canada and CANARIE; Chinese Academy of Sciences and research Grant No. QYZDJ-SSW-SLH011, National Natural Science Foundation of China and research Grants No. 11521505, No. 11575017, No. 11675166, No. 11761141009, No. 11705209, and No. 11975076, LiaoNing Revitalization Talents Program under Contract No. XLYC1807135, Shanghai Pujiang Program under Grant No. 18PJ1401000, and the CAS Center for Excellence in Particle Physics (CCEPP); the Ministry of Education, Youth, and Sports of the Czech Republic under Contract No. LTT17020 and Charles University Grant No. SVV 260448 and the Czech Science Foundation Grant No. 22-18469S; European Research Council, Seventh Framework PIEF-GA-2013-622527, Horizon 2020 ERC-Advanced Grants No. 267104 and No. 884719, Horizon 2020 ERC-Consolidator Grant No. 819127, Horizon 2020 Marie Sklodowska-Curie Grant Agreement No. 700525 "NIOBE" and No. 101026516, and Horizon 2020 Marie Sklodowska-Curie RISE project JENNIFER2 Grant Agreement No. 822070 (European grants); L'Institut National de Physique Nucléaire et de Physique des Particules (IN2P3) du CNRS (France); BMBF, DFG, HGF, MPG, and AvH Foundation (Germany); Department of Atomic Energy under Project Identification No. RTI 4002 and Department of Science and Technology (India); Israel Science Foundation Grant No. 2476/17, U.S.-Israel Binational Science Foundation Grant No. 2016113, and Israel Ministry of Science Grant No. 3-16543; Istituto Nazionale di Fisica Nucleare and the research grants BELLE2; Japan Society for the Promotion of Science, Grant-in-Aid for Scientific Research Grants No. 16H03968, No. 16H03993, No. 16H06492, No. 16K05323, No. 17H01133, No. 17H05405, No. 18K03621, No. 18H03710, No. 18H05226, No. 19H00682, No. 22H00144, No. 26220706, and No. 26400255, the National Institute of Informatics, and Science Information NETwork 5 (SINET5), and the Ministry of Education, Culture, Sports, Science, and Technology (MEXT) of Japan; National Research Foundation (NRF) of Korea Grants No. 2016R1D1A1B02012900, No. 2018R1A2B3003643, No. 2018R1A6A1A06024970, No. 2018R1D1A1B07047294, No. 2019R1I1A3A01058933, No. 2022R1A2C1003993, and No. RS-2022-00197659, Radiation Science Research Institute, Foreign Large-Size Research Facility Application Supporting project, the Global Science Experimental Data Hub Center of the Korea Institute of Science and Technology Information and KREONET/GLORIAD; Universiti Malaya RU grant, Akademi Sains Malaysia, and Ministry of Education Malaysia; Frontiers of Science Program Contracts No. FOINS-296, No. CB-221329, No. CB-236394, No. CB-254409, and No. CB-180023, and No. SEP-CINVESTAV research Grant No. 237 (Mexico); the Polish Ministry of Science and Higher Education and the National Science Center; the Ministry of Science and Higher Education of the Russian Federation, Agreement No. 14.W03.31.0026, and the HSE University Basic Research Program, Moscow; University of Tabuk research Grants No. S-0256-1438 and No. S-0280-1439 (Saudi Arabia); Slovenian Research Agency and research Grants No. J1-9124 and No. P1-0135; Agencia Estatal de Investigacion, Spain Grant No. RYC2020-029875-I and Generalitat Valenciana, Spain Grant No. CIDEGENT/2018/020 Ministry of Science and Technology and research Grants No. MOST106-2112-M-002-005-MY3 and No. MOST107-2119-M-002-035-MY3, and the Ministry of Education (Taiwan); Thailand Center of Excellence in Physics; TUBITAK ULAKBIM (Turkey); National Research Foundation of Ukraine, Project No. 2020.02/0257, and Ministry of Education and Science of Ukraine; the U.S. National Science Foundation and research Grants No. PHY-1913789 and No. PHY-2111604, and the U.S. Department of Energy and research Awards No. DE-AC06-76RLO1830, No. DE-SC0007983, No. DE-SC0009824, No. DE-SC0009973, No. DE-SC0010007, No. DE-SC0010073, No. DE-SC0010118, No. DE-SC0010504, No. DE-SC0011784, No. DE-SC0012704, No. DE-SC0019230, No. DE-SC0021274, No. DE-SC0022350; and the Vietnam Academy of Science and Technology (VAST) under Grant No. DL0000.05/21-23. These acknowledgements are not to be interpreted as an endorsement of any statement made by any of our institutes, funding agencies, governments, or their representatives. We thank the SuperKEKB team for delivering high-luminosity collisions; the KEK cryogenics group for the efficient operation of the detector solenoid magnet; the KEK computer group and the NII for on site computing support and SINET6 network support; and the raw-data centers at BNL, DESY, GridKa, IN2P3, INFN, and the University of Victoria for off site computing support.

[1] M. Neubert, Adv. Ser. Dir. High Energy Phys. **15**, 239 (1998).
[2] N. Uraltsev, in *At the frontier of Particle Physics*, edited by M. Shifman and B. Ioffe (2001), 10.1142/9789812810458_0034.

[3] A. Lenz and T. Rauh, Phys. Rev. D **88**, 034004 (2013).
[4] A. Lenz, Int. J. Mod. Phys. A **30**, 1543005 (2015).
[5] M. Kirk, A. Lenz, and T. Rauh, J. High Energy Phys. 12 (2017) 068; 06 (2020) 162(E).
[6] H.-Y. Cheng, J. High Energy Phys. 11 (2018) 014.
[7] J. Gratrex, B. Melić, and I. Nišandžić, J. High Energy Phys. 07 (2022) 058.
[8] R. Aaij *et al.* (LHCb Collaboration), Phys. Rev. Lett. **121**, 092003 (2018).
[9] R. Aaij *et al.* (LHCb Collaboration), Phys. Rev. D **100**, 032001 (2019).
[10] R. Aaij *et al.* (LHCb Collaboration), Sci. Bull. **67**, 479 (2022).
[11] P. A. Zyla *et al.* (Particle Data Group), Prog. Theor. Exp. Phys. **2020**, 083C01 (2020).
[12] J. M. Link *et al.* (FOCUS Collaboration), Phys. Rev. Lett. **88**, 161801 (2002).
[13] A. Kushnirenko *et al.* (SELEX Collaboration), Phys. Rev. Lett. **86**, 5243 (2001).
[14] A. H. Mahmood *et al.* (CLEO Collaboration), Phys. Rev. Lett. **86**, 2232 (2001).
[15] F. Abudinén *et al.* (Belle II Collaboration), Phys. Rev. Lett. **127**, 211801 (2021).
[16] T. Abe *et al.* (Belle II Collaboration), arXiv:1011.0352.
[17] K. Akai, K. Furukawa, and H. Koiso, Nucl. Instrum. Methods Phys. Res., Sect. A **907**, 188 (2018).
[18] S. Jadach, B. F. L. Ward, and Z. Was, Comput. Phys. Commun. **130**, 260 (2000).
[19] T. Sjöstrand, S. Ask, J. R. Christiansen, R. Corke, N. Desai, P. Ilten, S. Mrenna, S. Prestel, C. O. Rasmussen, and P. Z. Skands, Comput. Phys. Commun. **191**, 159 (2015).
[20] D. J. Lange, Nucl. Instrum. Methods Phys. Res., Sect. A **462**, 152 (2001).
[21] S. Agostinelli *et al.* (GEANT4 Collaboration), Nucl. Instrum. Methods Phys. Res., Sect. A **506**, 250 (2003).
[22] T. Kuhr, C. Pulvermacher, M. Ritter, T. Hauth, and N. Braun (Belle II Framework Software Group), Comput. Softw. Big Sci. **3**, 1 (2019).
[23] V. Bertacchi *et al.* (Belle II Tracking Group), Comput. Phys. Commun. **259**, 107610 (2021).
[24] S. Kurz, *Proceedings, Connecting the Dots 2020*, PROC-CTD2020-40, BELLE2-CONF-PROC-2020-009, https://docs.belle2.org/record/1960.
[25] J.-F. Krohn *et al.* (Belle II Analysis Software Group), Nucl. Instrum. Methods Phys. Res., Sect. A **976**, 164269 (2020).
[26] T. Lesiak *et al.* (Belle Collaboration), Phys. Lett. B **605**, 237 (2005).
[27] R. Aaij *et al.* (LHCb Collaboration), Phys. Rev. D **102**, 071101 (2020).
[28] P.-Y. Niu, Q. Wang, and Q. Zhao, Phys. Lett. B **826**, 136916 (2022).
[29] N. L. Johnson, Biometrika **36**, 149 (1949).
[30] T. Bilka *et al.*, EPJ Web Conf. **245**, 02023 (2020).